

CLOUD CAVITATION ON AN OSCILLATING HYDROFOIL

G. E. Reisman, E. A. McKenney, and C. E. Brennen
California Institute of Technology
Pasadena, CA

Presented at:

The Twentieth Symposium on Naval Hydrodynamics
Office of Naval Research
National Research Council

Santa Barbara, CA
August 21-26, 1994

CLOUD CAVITATION ON AN OSCILLATING HYDROFOIL

G. E. Reisman, E. A. McKenney, and C. E. Brennen
California Institute of Technology
Pasadena, CA

ABSTRACT

Cloud cavitation, often formed by the breakdown and collapse of a sheet or vortex cavity, is believed to be responsible for much of the noise and erosion damage that occurs under cavitating conditions. For this paper, cloud cavitation was produced through the periodic forcing of the flow by an oscillating hydrofoil. The present work examines the acoustic signal generated by the collapse of cloud cavitation, and compares the results to those obtained by studies of single travelling bubble cavitation. In addition, preliminary studies involving the use of air injection on the suction surface of the hydrofoil explore its mitigating effects on the cavitation noise.

NOMENCLATURE

c = Chord length of foil (m)
 I = Acoustic impulse ($Pa \cdot s$)
 I^* = Dimensionless acoustic impulse
 k = Reduced frequency = $\omega c/2U$
 p = Test section absolute pressure (Pa)
 \bar{p} = Time averaged pressure (Pa)
 p_a = Radiated acoustic pressure (Pa)
 p_A = Acoustic pressure intensity (Pa)
 p_v = Vapor pressure of water (Pa)
 q = Normalized air flow rate = Q/Ucs
 Q = Volume flow rate of air at test section pressure and temperature (m^3/sec)
 \mathcal{R} = Distance between noise source and hydrophone (m)
 s = Span of foil (m)
 t = Time (s)
 T = Period of foil oscillation (s)
 U = Tunnel test section velocity (m/s)
 V = Volume of cavitation bubble or cloud (m^3)
 α = Instantaneous angle of attack of foil (deg)
 $\bar{\alpha}$ = Mean angle of attack of foil (deg)
 ρ = Fluid density (kg/m^3)
 σ = Cavitation number = $(p - p_v)/\frac{1}{2}\rho U^2$
 ω = Foil oscillation frequency (rad/s)

INTRODUCTION

In many flows of practical interest one observes the periodic formation and collapse of a "cloud" of cavitation bubbles. The cycle may occur naturally as a result of the shedding of bubble-filled vortices, or it may be the response to a periodic disturbance imposed on the flow. Common examples of imposed fluctuations are the interaction between rotor and stator blades in a pump or turbine and the interaction between a ship's propeller and the non-uniform wake created by the hull. In many of these cases the coherent collapse of the cloud of bubbles can cause more intense noise and more potential for damage than in a similar non-fluctuating flow. A number of investigators (Bark and van Berlekom [1], Shen and Peterson [2], Bark [3], Franc and Michel [4] and Kubota *et al.* [5, 6]) have studied the complicated flow patterns involved in the production and collapse of a cavitating cloud on a hydrofoil. The present paper represents a continuation of these studies.

Previous studies have shown that, as an attached cavity collapses and is shed into the wake, the breakup of the cavity often results in the occurrence of cloud cavitation. The structure of such clouds appears to contain strong vortices, perhaps formed by the shear layer at the surface of the collapsing cavity (see Kubota *et al.* [5], Maeda *et al.* [7]). These clouds then collapse with some violence, often causing severe erosion on the surface and generating significant amounts of noise (Bark and van Berlekom [1], Kato [8], Ye *et al.* [9]). Figure 1 shows two typical examples of cloud cavitation on the oscillating hydrofoil used in the current study.

One of the present goals was to relate the characteristics of the acoustic signature of a cavitating cloud to the dynamics of the associated collapse process. The details of the cavity growth and collapse and cloud formation are discussed by previous authors, including McKenney and Bren-

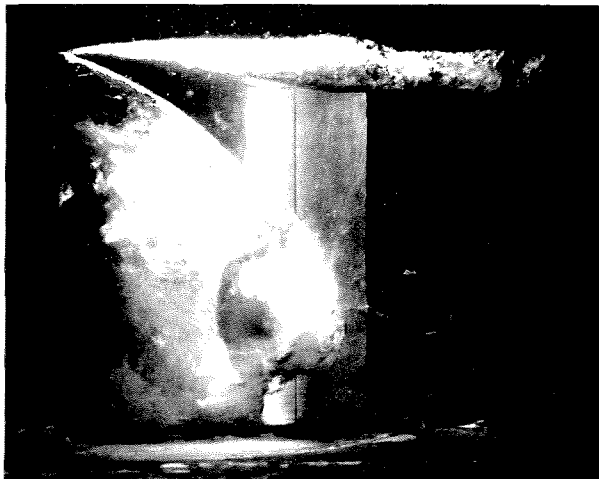


Figure 1: Cloud cavitation on an oscillating hydrofoil. The photograph on the left is without air injection, $\sigma = 1.2$, $k = 0.9$, $\alpha = 10.3^\circ$ (α decreasing). The photograph on the right has a normalized air flow rate of $q = 2.2 \times 10^{-4}$, with $\sigma = 1.2$, $k = 0.8$, $\alpha = 7.4^\circ$ (α decreasing).

nen [10]. Briefly, the cycle begins with the formation of travelling bubble cavitation near the leading edge of the foil as illustrated in figure 2. As the angle of attack increases, the bubbles grow and coalesce to form a single sheet cavity attached to the leading edge, as seen in figure 13. The downstream edge of this cavity is unstable and soon breaks down into a cloud of froth. In many cases a “sub-cloud” of the froth is ejected and travels downstream separately, with the main sheet cavity collapsing behind it. This sub-cloud is sometimes very coherent and may persist well after the remains of the sheet cavity have dispersed. The sub-cloud is believed to be the major source of the cavitation noise and its accompanying erosion.

As described by McKenney and Brennen [10], once the sub-cloud has travelled past the trailing edge of the foil there is a brief period in which there is no cavitation before the cycle begins again. A notable difference between those earlier experiments and the present work, however, is the hydrofoil mean angle of attack. In the previous work, the foil angle varied between 0° and 10° . Here, the angle of attack varies from 4° to 14° , so that even as the cloud from one cavitation cycle is dispersing a new sheet cavity has already begun to form at the leading edge. The photograph in figure 2 illustrates this overlap. Other than this, however, it appears that the sequence of events in the cavitation cycle



Figure 2: Between cavitation cycles: the cloud at the right is collapsing and beginning to disperse, while travelling bubble cavitation can already be seen near the leading edge just prior to forming a new sheet cavity. $\sigma = 1.0$, $k = 0.8$, $TAC = 4 - 5ppm$, $\alpha = 7.9^\circ$ (α increasing).

is very similar in the current experiments to those described previously.

The present paper will focus on the noise generated by the collapse of cavitating clouds and its dependence on various parameters. These results

will then be related to the existing knowledge of the generation of noise by a single collapsing cavitation bubble. Our traditional understanding of single bubble noise stems from the work of Fitzpatrick and Strasberg [11] and others (see, for example, Blake [12]) and is based on the Rayleigh-Plesset analysis of the dynamics of a spherical bubble. The radiated acoustic pressure, p_a , at a large distance, \mathcal{R} , from the center of a bubble of volume $V(t)$ is given by Blake [12]

$$p_a = \frac{\rho}{4\pi\mathcal{R}} \frac{d^2V}{dt^2}$$

Clearly a large positive noise pulse will be generated at the bubble collapse, due to the very large and positive values of d^2V/dt^2 that occur when the bubble is close to its minimum size. A good measure of the magnitude of the collapse pulse is the *acoustic impulse*, I , defined as the area under the pulse or

$$I = \int_{t_1}^{t_2} p_a dt$$

where t_1 and t_2 are chosen in a systematic manner to identify the beginning and end of the pulse. It is also useful in the present context to define a dimensionless impulse, I^* , as

$$I^* = \frac{16\pi I \mathcal{R}}{\rho U L^2}$$

where \mathcal{R} is now the distance from the cavitation event to the point of noise measurement and L is the typical dimension of the flow, taken in the present paper to be the chord of the foil.

Recently, both Ceccio and Brennen [13] and Kuhn de Chizelle *et al.* [14] were able to identify from within hydrophone data the acoustic signatures produced by the collapse of single travelling cavitation bubbles. They could thus measure the actual acoustic impulses of these events and compare them with the predictions of the Rayleigh-Plesset-Fitzpatrick-Strasberg theory for spherical bubbles. In general the measured values are about an order of magnitude smaller than the spherical bubble theory (see figure 8). The experiments also involved studies of the bubble shape distortions caused by the flow. Consequently it was possible to demonstrate that the reduction in the actual noise was correlated with the shape distortion. Crudely, one can visualize that a spherical collapse will be the most efficient noise-producing process since the collapse is focussed at a single point; thus any distortion in the sphericity of the bubble is likely to

defocus the collapse and reduce the noise. In the present paper we shall compare the impulses resulting from cloud collapses with those of the above-mentioned measurements of single bubble impulses in an attempt to learn more about the dynamics and acoustics of clouds of bubbles.

A similar study was performed on acoustic signals generated by cloud cavitation (McKenney and Brennen [10]), where it was qualitatively shown that the major acoustic burst in each cycle seems to correspond to the collapse of the cloud cavitation. The long-term goal in all these acoustic studies is not only to gain an understanding of the flow mechanisms that produce the noise, but also to develop methods to reduce that noise and the erosive damage that generally accompanies it. It has been shown for the case of single bubble cavitation (Brennen [15]) that the presence of a contaminant gas reduces the rate of collapse and increases the minimum bubble volume. Thus one mitigation strategy is the deliberate injection of air to help "cushion" the collapse, thereby reducing the noise and damage potential. Several previous investigations have explored this strategy by ejecting air from ventilation holes in the suction surface of a hydrofoil. Ukon [16] used air injection from the leading edge of a stationary foil and found a consistent reduction in the noise in the frequency range 0.6 to 100kHz. The maximum noise reduction achieved was of the order of 20dB. There is some suggestion in his data that air flow rates above a certain optimal level no longer decrease the noise. Arndt *et al.* [17] performed similar air injection tests with a stationary foil and found some reduction in the mean square hydrophone signal in the 10 to 30Hz band. The reduction was a factor of approximately 3 to 5 for small air flow rates, but there was little additional effect at higher flow rates (see figure 11). In the present experiments we also explore the noise reduction due to air flow rate, normalized as $q = Q/Ucs$.

EXPERIMENTAL APPARATUS

The Caltech Low Turbulence Water Tunnel is a closed-circuit facility, with a 30.5cm × 30.5cm × 2.5m test section. It is capable of freestream velocities up to 10m/s and can support pressures down to 20kPa. A complete description of this facility may be found in Gates [18]. The total air content (TAC) of the water in the tunnel was measured using a Van Slyke apparatus.

An NACA 64A309 hydrofoil was reflection-plane mounted in the test section, as shown in figure 3 and described in Hart *et al.* [19]. The hydrofoil

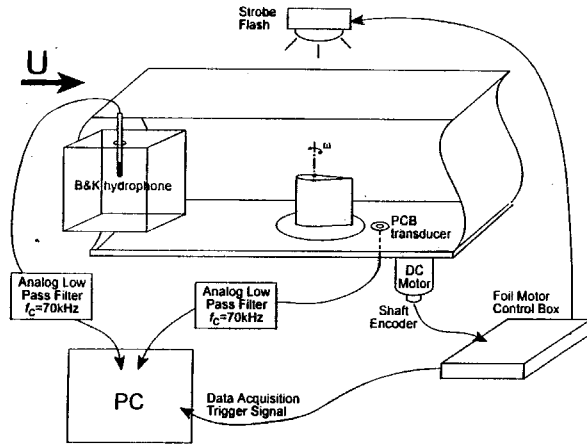


Figure 3: Oscillating hydrofoil in the water tunnel test section.

has a rectangular planform with a chord of 15.2cm and a span of 17.5cm ; it is made of stainless steel and polished to a smooth finish. It is connected to a 750 watt DC motor by a four-bar linkage such that it oscillates nearly sinusoidally in pitch about a point near the center of pressure, $0.38c$ from the leading edge. The mean angle of attack and the oscillation amplitude can be adjusted, and the oscillation frequency may be continuously varied from 0 to 50Hz . An optical shaft encoder mounted to the DC motor provides a digital signal (1024 pulses per revolution) which was used to synchronize acoustic measurements with the phase of the foil.

The sound generated by the cavitation on the hydrofoil was recorded using two transducers. A PCB model HS113A21 piezo-electric pressure transducer (bandwidth 100kHz) was mounted flush with the floor of the test section, approximately 5cm downstream of the trailing edge of the foil. In addition, a B&K model 8103 hydrophone (bandwidth 100kHz) was installed in a Lucite box filled with water and affixed tightly to the outside of the test section. As graphically demonstrated by Bark and van Berlekom [1], mounting a hydrophone externally in this way significantly degrades the signal. Analysis of the current data was used to compare results from these two transducers, with the following specific comments:

- The lucite box mounting approach is a sim-

ple way to obtain preliminary qualitative information. This method was used successfully by McKenney and Brennen [10] to correlate the cloud cavitation acoustics with high-speed motion pictures of the collapse.

- Acoustic pressure intensities calculated using the output from the hydrophone in the box were significantly smaller in magnitude than those derived from the flush-mounted transducer for the same event, generally by a factor of 2 or 3. This indicates that the presence of the walls of the test section and the lucite box has a severely attenuating effect on the measured signal.
- Although the PCB transducer lacks the omnidirectional capability of the B&K hydrophone, the transducer was mounted directly beneath the cloud collapse region and thus the radiated acoustic pressure impinges with normal incidence.
- The PCB transducer produced results with greater scatter, but better signal to noise ratio. The signal for the external hydrophone was significantly adulterated by resonances within the box.

These conclusions are very similar to those reached by Bark and van Berlekom [1], and led to the decision to focus on the results obtained with the PCB (flush-mounted) transducer.

The output signals from both transducers were low pass filtered prior to being recorded by a digital data acquisition system. Since the sampling rate was approximately 143kHz , the filters were set to a cutoff frequency of 70kHz , just below the Nyquist frequency. The data acquisition system also recorded timing information from the oscillation of the foil.

Still photographs were taken of various stages of the cavitation process by using the foil timing to trigger strobe lighting at the desired phase of the foil oscillation cycle.

For the air injection studies, four holes were drilled in the suction surface of the foil, located at the axis of rotation and equally spaced along the span. The air flow rate was measured to within a 12% error by using an orifice flow meter. For the current studies, the injection flow rate was kept constant at levels which preliminary tests showed would produce a finite effect.

EXPERIMENTAL PROCEDURES

Experiments were conducted in the following parameter ranges:

Mean angle of attack, $\bar{\alpha}$	9°
Oscillation amplitude, $\Delta\alpha$	$\pm 5^\circ$
Reduced frequency, k	0.55 to 0.93
Cavitation number, σ	0.9 to 1.5
Air content (ppm)	4 to 10
Normalized air injection, q	0 to 10^{-3}

Data for about 40 cycles were obtained at each condition and in selected cases still photographs were taken. Figure 4 shows a typical signal before high-pass filtering, along with a curve indicating the foil instantaneous angle of attack during one oscillation cycle. The origin of the time axis corresponds to $\alpha = 7.9^\circ$ where α is increasing. The photograph in figure 2 was taken at the origin of the time axis in figure 4. Two clear pulses at about $\alpha = 10^\circ$ represent the sound produced by the cloud collapse in this particular cycle. The multiple peaks seen in this signal are characteristic of many of the signals obtained in these experiments. The presence of multiple peaks may suggest the formation of more than one cloud during the collapse of the main cavity, or it may be the result of the rebound and recollapse of a single cloud.

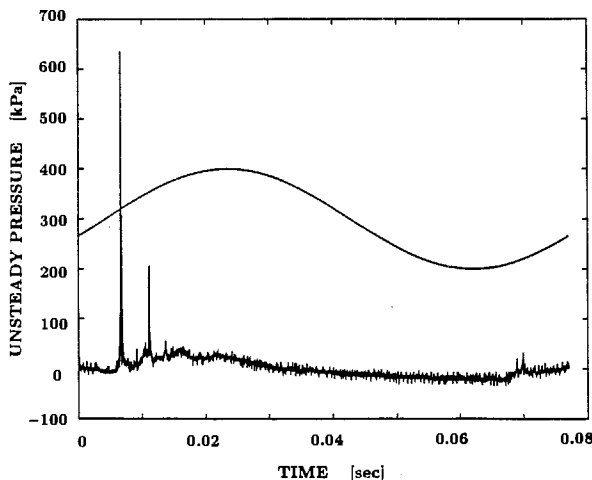


Figure 4: Typical output from the piezo-electric transducer. The signal from one oscillation cycle is shown together with a sinusoid qualitatively representing the instantaneous angle of attack of the foil. Data for $\sigma = 1.0$, $k = 0.8$, $TAC = 4 - 5ppm$.

The total air content was also measured before and after each run. For most of the experiments, the TAC was in the range of 8 – 10ppm. Then the water was deaerated so that the TAC was in the range 4 – 5ppm, and measurements were taken again at a few of the previous conditions.

We now turn to a discussion of the measurements of the noise generated by these flows. In the previous experiments, the sound level was evaluated by calculating the *acoustic pressure intensity*, which was measured over a whole oscillation cycle and nondimensionalized as follows:

$$p_A^* = \frac{p_A \mathcal{R}}{\frac{1}{2} U^2 c} \quad \text{where} \quad p_A = \left[\frac{1}{T} \int_0^T (p(t) - \bar{p})^2 dt \right]^{\frac{1}{2}}$$

This is related to the acoustic intensity defined in Coates [20] as $p_A^2 / \rho c^*$, where c^* is the speed of sound in the fluid.

For the current experiments, in part to facilitate comparing our results with those of researchers studying single travelling bubble acoustics, we calculated the acoustic impulse by integrating only over the distinct peaks in the signal, thus neglecting low-frequency variations in pressure as well as high-frequency but low-amplitude noise. The digitized signal from a single foil oscillation cycle was first high-pass filtered in software with a cutoff frequency of 50Hz to remove the low frequency pressure changes due to the foil motion. Choosing the limits of integration for the impulse calculations proved to be a non-trivial procedure; results may depend heavily on irrelevant artifacts in the data if the limits are poorly chosen. The method used by Kumar [21] and Ceccio [22] was selected, both for its robustness and its similarity of application to the current data. The beginning of a peak was identified by the positive-going signal crossing a threshold value of 20kPa. The end of the peak was defined as the moment when the signal crossed that same threshold value with a negative slope.

In addition, the spectra of the acoustic signals were compared under the different flow conditions. Average spectra from approximately 40 individual (unfiltered) cycles were acquired as follows: first the spectrum from each raw signal was normalized by the area under that spectrum following the method described in Kumar [21], then the normalized magnitudes at each frequency were averaged over all the cycles.

ACOUSTIC IMPULSE RESULTS

The experimental results depicted in figures 5, 6, and 7 illustrate the variation of the dimensionless impulse, I^* , with cavitation number, total air content, and reduced frequency. Each data point in these figures represents the average of approximately 40 cycles and the associated impulses. Within the parameter space, significant cycle-to-cycle variation was observed in both the physical attributes of the cavitation and the resulting impulse. A measure of this scatter is depicted in figure 5 and 6 by vertical bars which represent one standard deviation above and below the average impulse value. As demonstrated in these two figures, the standard deviation ranges from approximately 60% of the mean for dimensionless impulses greater than 0.4 to 120% of the mean for I^* less than 0.4. However it is important to observe that the repeatability of the mean value was approximately ± 0.1 .

Figures 5 and 7 show the change in impulse with reduced frequency, k , for different cavitation numbers. As expected, the cavitation number, σ , and reduced frequency, k , have a significant effect on the measured impulse, but no simple relationship between either of these two parameters and the impulse is evident. The highest cavitation number, $\sigma = 1.5$, resulted in the lowest impulse for all but one value of k . With the same exception, the sound level produced at $\sigma = 1.2$ exceeded the level measured at $\sigma = 0.9$. This reduction in sound level was also readily detectable in the laboratory as the cavitation number was lowered from 1.2 to 0.9. Thus, in general, the noise appears to peak at some intermediate σ .

This non-monotonic effect with cavitation number differs from that found by McKenney and Brennen [10], perhaps because the present mean angle of attack, $\bar{\alpha}$, is larger. This seems to alter the cavitation number at which the noise peaks. In the present experiments, it was observed visually during the experiments that for $\sigma = 0.9$ the sheet cavity not only covered nearly the entire surface of the hydrofoil, but also extended past the trailing edge for a large part of the oscillation cycle. At the lower $\bar{\alpha}$ in the earlier work, however, the sheet cavity seldom covered more than about 60% of the foil surface.

Although the total air content (TAC) varied from 4ppm to 10ppm during the experiments, it appeared to have little effect on the noise, as shown in figure 6.

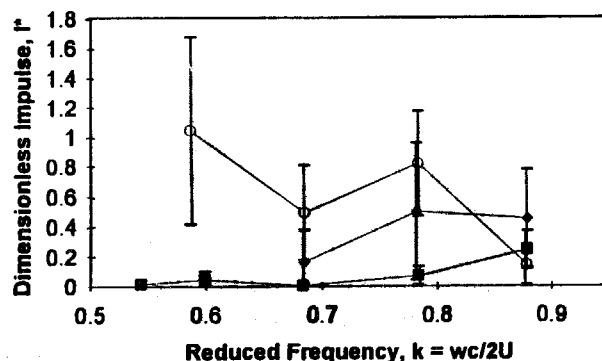


Figure 5: Effect of cavitation number, σ , on the dimensionless impulse, I^* . Data shown for $\sigma = 0.9$ (\blacklozenge), $\sigma = 1.2$ (\circ), $\sigma = 1.5$ (\blacksquare) with $TAC = 7 - 10ppm$.

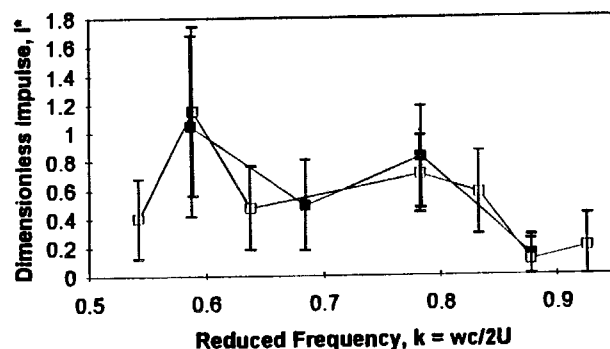


Figure 6: Effect of total air content (TAC) on dimensionless impulse, I^* . Data shown for $TAC = 4 - 5ppm$ (\square), $TAC = 8 - 10ppm$ (\blacksquare) with $\sigma = 1.2$.

Figure 7 presents a summary of the results for the averaged acoustic impulses and shows the variations with reduced frequency, cavitation number, and TAC. The results for the air injection experiments are also included in this figure and will be discussed in greater detail later.

It is interesting to compare the results for the acoustic impulse (depicted in figure 7) with previous results for single travelling bubbles. Figure 8 illustrates the approximate relations between the cloud cavitation impulses, the impulses observed by Kuhn de Chizelle *et al.* [14] for single travelling bubbles, and the impulse magnitudes predicted by the Rayleigh-Plesset equation for a spherical bubble. From this figure, it is evident that the noise generated by cloud cavitation is several orders of

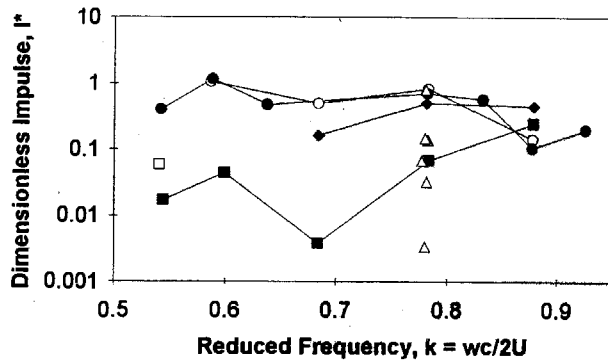


Figure 7: Summary of dimensionless impulse data for cloud cavitation. Data without air injection: $\sigma = 0.9$, $TAC = 7 - 8ppm$ (\blacklozenge); $\sigma = 1.2$, $TAC = 4 - 5ppm$ (\bullet); $\sigma = 1.2$, $TAC = 8 - 10ppm$ (\circ); $\sigma = 1.5$, $TAC = 4 - 5ppm$ (\square); $\sigma = 1.5$, $TAC = 9 - 10ppm$ (\blacksquare); Data with air injection: $\sigma = 1.2$, $TAC = 4 - 10ppm$ (\triangle).

magnitude larger than the sound level resulting from single travelling bubble cavitation. The impulses generated by some clouds are even greater than the theoretical prediction for a single spherical bubble of the same maximum volume. The figure suggests that clouds can be even more effective noise sources than single bubbles of the same volume. A possible explanation for this is the formation of an inwardly propagating shock wave within the collapsing cloud as originally suggested by Mørch [23] and recently demonstrated theoretically by Wang and Brennen [24].

SPECTRAL ANALYSIS

Further insight into cloud cavitation noise generation can be obtained by Fourier analysis of the radiated acoustic pressure. Figures 9 and 10 are two typical examples of cloud cavitation spectra. Each line in the figure corresponds to a single set of parameters and represents an average of approximately 40 Fourier transforms normalized using the method described above. The spectra obtained from the current experiments exhibit a characteristic behavior proportional to f^{-n} over the frequency range of $80 - 6000Hz$, where $0.7 > n > 0.8$. This compares reasonably well with the f^{-1} behavior of previous experimental results for single bubbles and for steady cavitating flows [15].

Figure 9 presents the averaged spectra for each

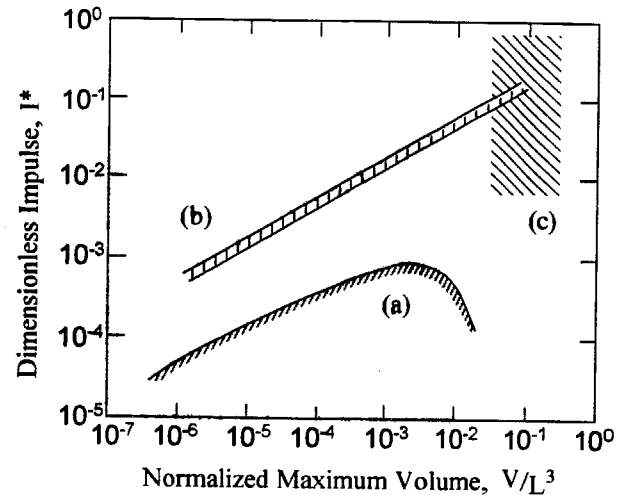


Figure 8: Acoustic impulse magnitude ranges as a function of the maximum bubble or cloud volume, for (a) single travelling bubble cavitation (Kuhn de Chizelle *et al.* [14]), (b) the Rayleigh-Plesset spherical bubble model for the conditions of the aforementioned experiments, and (c) cloud cavitation results from the present experiments.

of the three cavitation numbers. It is clear that there is a significant change in the spectrum with cavitation number particularly in the range from $100Hz$ to $5kHz$. Moreover, the changes in magnitude in this range correspond with previously described changes in the acoustic impulse with σ .

The large peak in the spectra at $9kHz$ appears for every data set in the entire parameter space. When the impulse response of the test section was measured, it indicated peaks at approximately 4 , 32 , and $64kHz$, but the response was flat in the frequency range near $9kHz$. Since the location and relative magnitude of the $9kHz$ peak shows no appreciable variation with the various flow parameters, cavitation noise is an unlikely explanation.

Another interesting feature of figure 9 is the presence of peaks at approximately $3kHz$. Unlike those at $9kHz$, these peaks vary somewhat with cavitation number. It is possible that these represent the frequency of the large radiated pressure pulses associated with cloud cavitation, such as those seen in figure 4. Figure 10 shows how the frequency content of the sound changes with variation in the reduced frequency. The spectra are similar, except for the three peaks between 2 and $4kHz$, whose frequency increases with decreasing reduced frequency. Average spectra were also examined for different air contents, but showed little change with

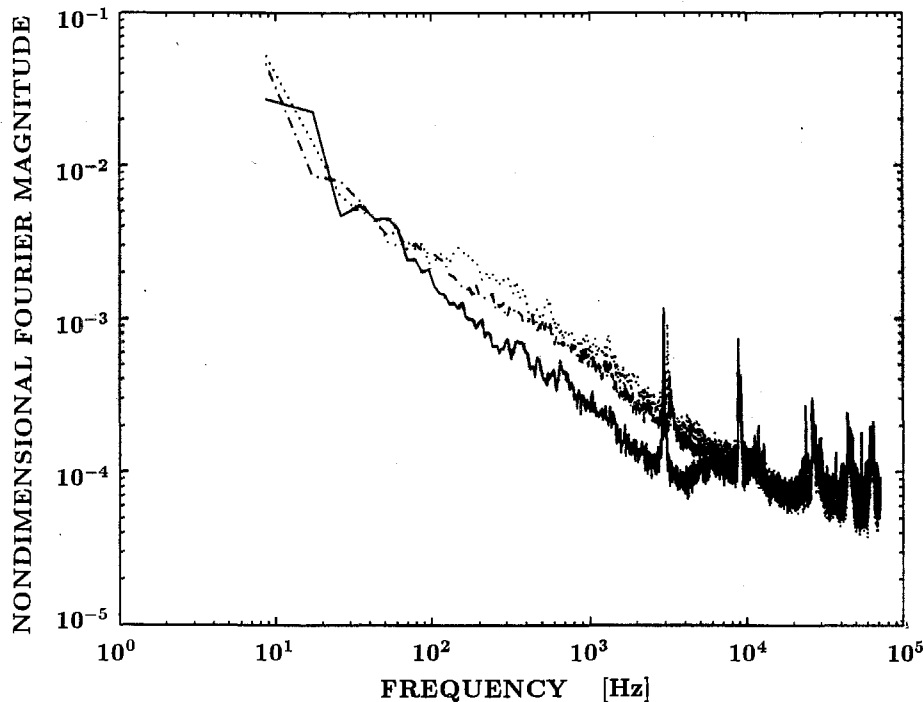


Figure 9: Comparison of the normalized spectra of unsteady pressures at three different cavitation numbers: $\sigma = 1.5$ (solid line), $\sigma = 1.2$ (dotted line), and $\sigma = 0.9$ (dash-dot line). Data for $k = 0.7$, $TAC = 7 - 10ppm$.

this parameter.

AIR INJECTION

Air injection resulted in a dramatic reduction in the sound level. At a sufficiently high air flow rate, the periodic “bangs” associated with cloud cavitation collapse could no longer be detected either by ear or by transducer. Figure 11 illustrates this noise reduction as a function of normalized air injection flow rate. Data from the current experiments are plotted along with results from work by Arndt, *et al.* [17] and Ukon [16]. The ordinates on this figure are the ratio of the sound pressure level at a given air flow rate to the sound pressure level without air injection. In this figure we have used the average impulses from the present experiments and the root mean squared acoustic pressure for the data from Arndt *et al.* and Ukon. We note that the present experimental data showed a very strong correlation between the impulse and the RMS acoustic pressure.

The experiments performed by Arndt *et al.* and

Ukon utilized stationary hydrofoils. Although cavitation clouds can separate periodically from sheet cavitation on a stationary foil, the collapse usually lacks the intensity of cloud cavitation caused by an imposed periodicity. The resulting low ratio of cavitation noise to background noise could explain the relatively small noise reduction due to air flow which is apparent in the data of Arndt *et al.*

In contrast, our observations indicate that the impulse could be reduced by a factor greater than 200 at an air flow rate, q , of approximately 0.001. At this flow rate, the periodic cloud cavitation noise was completely suppressed, and a further increase in the air flow rate had no discernible effect.

The spectral content of the cavitation noise also changed with air injection. Figure 12 shows the average normalized Fourier spectra for three different air flow rates. As the air injection flow rate is increased, the Fourier magnitudes in the frequency range between 100 Hz and 8 kHz decrease relative to the high and low frequency content.

Another effect of air injection was an increase in the average size of the sheet cavity. This phenomenon was previously noted by Ukon [16]. Al-

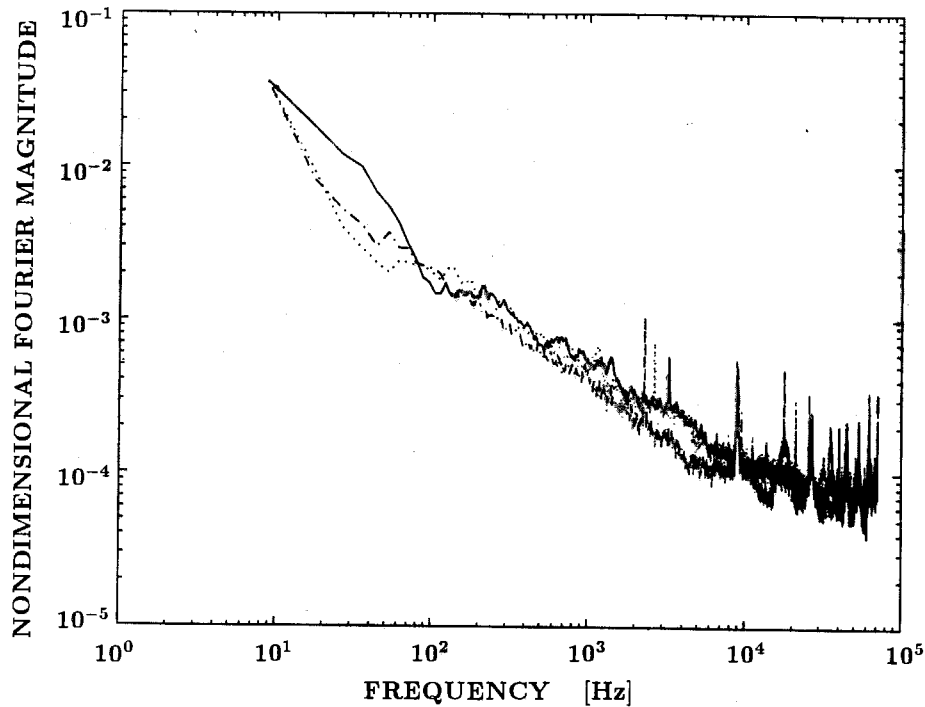


Figure 10: Comparison of the spectra of unsteady pressures at three different reduced frequencies: $k = 0.64$ (solid line), $k = 0.8$ (dotted line), and $k = 0.93$ (dash-dot line). Data for $\sigma = 1.2$, $TAC = 4 - 5ppm$.

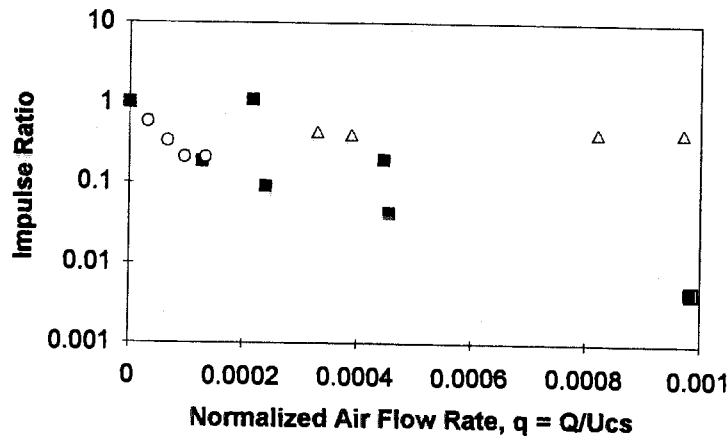


Figure 11: Effect of air flow rate on the radiated noise, normalized by the noise without air injection. Data for the current experiments at $\sigma = 1.2$, $k = 0.8$, $TAC = 5 - 10ppm$ are shown (\blacksquare), and compared with data from Ukon [16] at $\sigma = 0.74$, $\alpha = 6.4^\circ$, $U = 8m/s$ (\circ) and Arndt *et al.* [17] at $\sigma = 0.9$, $\alpha = 8^\circ$, $U = 15$ and $7.5m/s$ (\triangle).

though the two photographs in figure 13 were taken at identical cavitation numbers, reduced frequencies, and angles of attack, the cavity area is much larger in the air injection case. This effect is simply due to an increase in the mean pressure in the cavity and therefore a decrease in the effective cava-

tion number. Examination of the still photographs also shows that the added air also increases the size of the cloud generated when the sheet cavity collapses, as shown in figure 1. This rules out the possibility that the noise reduction is due to suppression of the cloud cavitation. Instead, it seems prob-

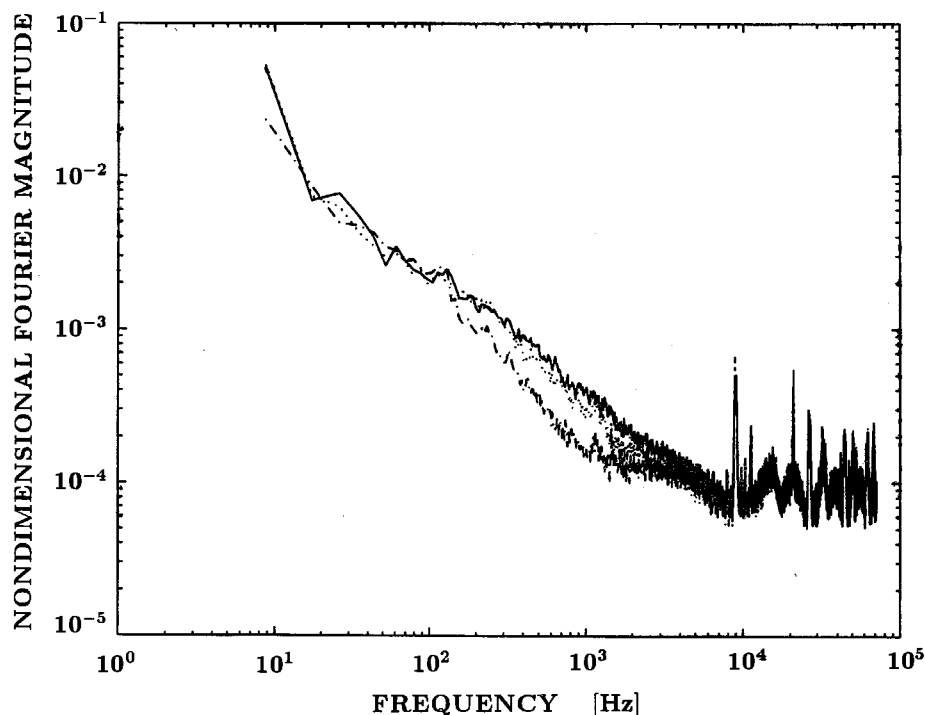


Figure 12: Effect of air injection on the spectral content of the noise for three normalized air flow rates: $q = 1.3 \times 10^{-4}$ (solid line), $q = 2.4 \times 10^{-4}$ (dotted line), $q = 9.8 \times 10^{-4}$ (dot-dash line). Data for $k = 0.8$, $TAC = 7 - 10ppm$.

able that the bubbles in the cloud contain more air, which cushions the collapse and reduces the overall sound produced.

CONCLUSIONS

This paper has examined the acoustic impulses produced by the collapse of clouds of cavitation bubbles. The clouds were generated by pitch oscillations of a finite aspect ratio hydrofoil in a water tunnel. The recorded noise was analyzed in several ways. First, large positive noise pulses were clearly present in the signal and corresponded to the collapse of clouds of bubbles shed by the foil. The acoustic impulses associated with these pulses were obtained by integration, and the variations with cavitation number, air content, and foil oscillation frequency were examined. The impulses appear to peak at the intermediate cavitation number studied and to be relatively independent of the air content. The variations with foil oscillation frequency are significant but not readily understood. We should also note that the impulses are consis-

tent with, though somewhat larger than, what had been expected from the extrapolation of data on single bubbles. This suggests the existence of an additional mechanism in the cloud collapse that augments the noise, such as an inwardly propagating shock.

Spectra of the noise, averaged over more than 40 cycles, were also examined and exhibited a typical f^{-1} variation with frequency. Significant variations in the shape with cavitation number could be discerned, however air content and foil oscillation frequency produced no such discernible variation.

Air injection from the suction surface of the foil was investigated and produced major reduction in the noise similar to the reductions earlier observed by Arndt *et al.* [17] and Ukon [16], though we also observed much larger reductions (up to a factor of 200) in the acoustic impulses than the reduction in RMS noise measured by those previous authors. Indeed the large pulses seem to be eliminated, leaving only the incoherent bubble collapse noise. Comparison of the photographs of the cavitation suggests that the mechanism for the noise

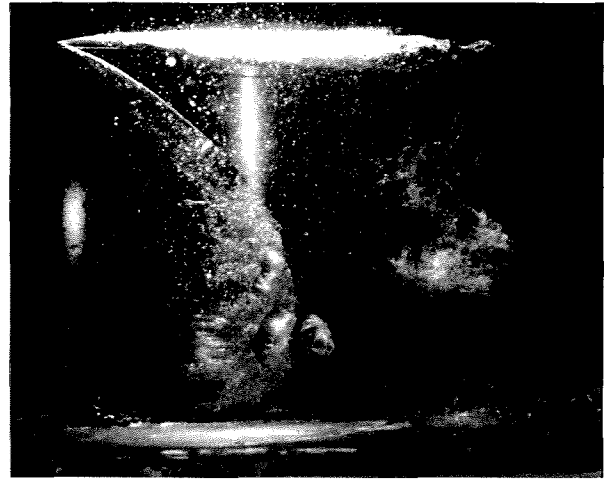


Figure 13: Effect of air injection on cavity size. The photograph on the left is without air injection, the photograph on the right has a normalized air flow rate of $q = 4.5 \times 10^{-4}$. Both photographs were taken at $\sigma = 1.2$, $k = 0.8$, $\alpha = 12.8^\circ$

reduction is an increase in the air contained in the bubbles which comprise the cloud. It also seems that air flow rates above a certain level produce no further reduction in the sound.

ACKNOWLEDGEMENTS

We wish to acknowledge our debt to Y.-C. Wang, J. Ando, F. d'Auria, T. Waniewski, R. and V. Zenit, and Z. Liu for help in conducting the experiments. Joe Fontana's machine shop assistance was greatly appreciated as well. The authors are grateful for the support of the Office of Naval Research under grant number N00014-91-J-1295.

References

- [1] Bark, G. and van Berlekom, W. B. (1978). Experimental investigations of cavitation noise. *Proc. 12th ONR Symp. on Naval Hydrodynamics*, pp. 470-493.
- [2] Shen, Y. and Peterson, F. B. (1978). Unsteady cavitation on an oscillating hydrofoil. *Proc. 12th ONR Symp. on Naval Hydrodynamics*, pp. 362-384.
- [3] Bark, G. (1985). Developments of distortions in sheet cavitation on hydrofoils. *Proc. ASME Int. Symp. on Jets and Cavities*, pp. 215-225.
- [4] Franc, J. P. and Michel, J. M. (1988). Unsteady attached cavitation on an oscillating hydrofoil. *J. Fluid Mech.*, Vol. 193, pp. 171-189.
- [5] Kubota, A., Kato, H., Yamaguchi, H., and Maeda, M. (1989). Unsteady structure measurement of cloud cavitation on a foil section using conditional sampling. *J. Fluids Eng.*, Vol. 111, pp. 204-210.
- [6] Kubota, A., Kato, H., and Yamaguchi, H. (1992). A new modelling of cavitating flows - a numerical study of unsteady cavitation on a hydrofoil section. *J. Fluid Mech.*, Vol. 240, pp. 59-96.
- [7] Maeda, M., Yamaguchi, H., and Kato, H. (1991). Laser holography measurement of bubble population in cavitation cloud on a foil section. *Proc. ASME Symp. on Cavitation*, Vol. 116, pp. 67-75.
- [8] Kato, H. (1985). On the structure of cavity: New insight into the cavity flow: A summary of the keynote speech. *Proc. of the ASME Int. Symp. on Jets and Cavities*, Vol. 31, pp. 13-19.

- [9] Ye, Y. P., Kato, H., and Maeda, M. (1989). On correlation of cavitation erosion and noise on a foil section. *Int. Workshop on Cavitation*, pp. 68–75, Wuxi, Jiangsu, China.
- [10] McKenney, E. A. and Brennen, C. E. (1994). On the dynamics and acoustics of cloud cavitation on an oscillating hydrofoil. *Proc. ASME Symp. on Cavitation and Gas-Liquid Flow in Fluid Machinery and Devices*.
- [11] Fitzpatrick, H. M. and Strasberg, M. (1956). Hydrodynamic sources of sound. *Proc. First ONR Symp. on Naval Hydrodynamics*, pp. 241–280.
- [12] Blake, W. K. (1986). *Mechanics of flow-induced sound and vibration*. Academic Press.
- [13] Ceccio, S. L. and Brennen, C. E. (1991). Observations of the dynamics and acoustics of travelling bubble cavitation. *J. Fluid Mech.*, Vol. 233, pp. 633–660.
- [14] Kuhn de Chizelle, Y., Ceccio, S. L., and Brennen, C. E. Observations, scaling and modelling of travelling bubble cavitation. Submitted for publication., 1994.
- [15] Brennen, C. E. (1994). *Cavitation and Bubble Dynamics*. Oxford University Press.
- [16] Ukon, Y. (1986). Cavitation characteristics of a finite swept wing and cavitation noise reduction due to air injection. *Proc. of the Int. Symp. on Propeller and Cavitation*, pp. 383–390.
- [17] Arndt, R. E. A., Ellis, C. R., and Paul, S. (1993). Preliminary investigation of the use of air injection to mitigate cavitation erosion. *Proc. ASME Symp. on Bubble Noise and Cavitation Erosion in Fluid Systems*, Vol. 176, pp. 105–116.
- [18] Gates, E. M. (1977). *The Influence of Freestream Turbulence, Freestream Nuclei Populations, and a Drag-Reducing Polymer on Cavitation Inception on Two Axisymmetric Bodies*. PhD thesis, Cal. Inst. of Tech.
- [19] Hart, D. P., Brennen, C. E., and Acosta, A. J. (1990). Observations of cavitation on a three-dimensional oscillating hydrofoil. *ASME Cavitation and Multiphase Flow Forum*, Vol. 98, pp. 49–52.
- [20] Coates, R. F. W. (1989). *Underwater Acoustic Systems*. John Wiley & Sons, Inc.
- [21] Kumar, S. (1991). *Some Theoretical and Experimental Studies of Cavitation Noise*. PhD thesis, Cal. Inst. of Tech.
- [22] Ceccio, S. L. (1990). *Observations of the Dynamics and Acoustics of Travelling Bubble Cavitation*. PhD thesis, Cal. Inst. of Tech.
- [23] Mørch, K. A. (1980). On the collapse of cavity cluster in flow cavitation. *Proc. First Int. Conf. on Cavitation and Inhomogeneities in Underwater Acoustics*, Vol. 4, pp. 95–100. Springer Series in Electrophysics.
- [24] Wang, Y.-C. and Brennen, C. E. (1994). Shock wave development in the collapse of a cloud of bubbles. *ASME Cavitation and Multiphase Flow Forum*, Vol. 153.